Context-dependent ATP7 Interactions with Parkinson's Disease-associated Genes Modulate Copper Homeostasis Phenotypes

Brooke M. Allen[1*], Nadia Gonzalez[2-3*], Erica Werner[4], Victor Faundez[4], and Alysia D. Vrailas-Mortimer[1-3, #]

1. Illinois State University, School of Biological Sciences, Normal, IL, USA
2. Oregon State University, Department of Biochemistry and Biophysics, Corvallis, OR, USA
3. Oregon State University, Linus Pauling Institute, Corvallis, OR, USA
4. Emory University, Department of Cell Biology, Atlanta, GA, USA

*Denotes equal contribution

Running Title: LRRK2 and Copper Homeostasis

Key words/phrases: LRRK2, ATP7, Copper Homeostasis, Parkinson's disease

Corresponding author:
Alysia D. Vrailas-Mortimer
Oregon State University
Department of Biochemistry and Biophysics
Corvallis, OR 97331
Phone: 541-737-9551
e-mail: Alysia.Mortimer@oregonstate.edu
ORCID: 0000-0001-5927-096X

Brooke Allen ORCID: 0009-0002-6028-3340
Nadia Gonzalez ORCID: 0009-0001-3889-6573
Erica Werner ORCID: 0000-0002-8183-16001
Victor Faundez ORCID: 0000-0002-2114-5271

32
33
34 **Summary Statement**
35 We performed a genetic interaction screen to explore the relationship between copper
36 homeostasis and Parkinson's disease and other neurodegeneration associated genes.
37
38 **Abstract**
39 Copper is an essential micronutrient required by enzymes that catalyze oxygen-dependent
40 reactions, but toxic in excess. Mutations in the ATP7A and ATP7B copper transporters cause
41 neuropsychiatric symptoms and neurodegeneration by mechanisms that remain to be elucidated.
42 We previously reported that the ATP7A biochemical interactome is enriched in Parkinson's
43 disease (PD) and neurodegeneration associated genes, yet the functional outcomes of these
44 interactions are unknown. Using *Drosophila,* we tested genetic interactions between ATP7
45 mutants that alter copper levels and a subset of these PD and neurodegeneration causative genes
46 and found sex differences with some candidate genes enhancing ATP7 deleterious phenotypes in
47 both sexes, while others were sex specific. Most notably, we found that Lrrk2 (Lrrk), the most
48 commonly mutated gene in familial forms of PD, protects against ATP7 dysfunction in
49 epidermal epithelial cells with a stronger effect in males than females. However, in dopaminergic
50 neurons Lrrk plays a role in intracellular copper induced toxicity in females but not males,
51 supporting context dependent interactions between ATP7A and PD-associated genes to protect
52 against disruptions in copper homeostasis.
53
54 **Introduction**
55 Copper is an essential micronutrient that acts as a structural component and catalytic cofactor for
56 key cellular processes, such as antioxidant defense, mitochondrial respiration, energy and iron
57 metabolism, and neurotransmitter production[1–3]. Disruptions in copper homeostasis can cause
58 oxidative damage and impaired function of critical cuproenzymes, resulting in cellular
59 dysfunction and cell death[4–6]. Therefore, copper homeostasis is tightly regulated within the cell
60 by the copper transporters ATP7A and B which pump cytoplasmic copper into the lumen of the
61 Golgi apparatus for metalation of secreted cuproenzymes. Excess levels of cytoplasmic copper,
62 cause ATP7A/B translocation to the plasma membrane, pumping excess copper out of the cell[7–

63 [10]. Thus, deficiencies in ATP7B leads to copper accumulation at the cellular level and at the
64 organism level, resulting in the neurodegenerative disorder Wilson's disease[5,6]. Whereas
65 ATP7A mutations can cause Menkes disease, a multi-system disorder that includes widespread
66 neurodegeneration caused by decreased copper in the brain due to defective dietary copper
67 absorption[10,11]. Similarly, in the fruit fly, *Drosophila melanogaster*, genetic manipulation of the
68 sole homologue *ATP7* causes a copper depletion phenotype affecting neuronal function[12] and
69 structure[13] and induces early mortality[14]. We have found that ATP7A interacts with proteins
70 associated with neurodegeneration and neurodevelopmental disorders[13], and ATP7A mutant
71 fibroblasts have altered expression of proteins associated with Parkinson's disease (PD) or
72 neurodegeneration, including elevated expression of the early onset neurodegenerative disease
73 protein, UCHL1[14]. Furthermore, we confirmed this link between ATP7 and UCHL1 through
74 genetic interactions in *Drosophila*[14].
75
76 PD is the second most common neurodegenerative disease and is characterized by loss of
77 dopaminergic neurons in the substantia nigra, impaired mitochondria, and increased oxidative
78 stress[15,16]. Familial forms of PD account for only 5-15% of cases, suggesting a strong
79 environmental component for this disease[15–17]. However, low brain copper levels can lead to
80 dysfunction and neurodegeneration as well, and copper levels are reduced in mice treated with
81 MPTP, a potent inducer of PD-like phenotypes[18,19]. Additionally, key mitochondrial proteins
82 such as Cytochrome c oxidase and superoxide dismutase (SOD1) are cuproenzymes, and ATP7A
83 mutant fibroblasts have impaired mitochondria[14,20]. Furthermore, both elevated and reduced
84 levels of copper can induce oxidative stress through different mechanisms[21,22], suggesting that
85 both increased and decreased levels of intracellular copper may contribute to PD. This is
86 supported by findings that administering $CuSO_4$ or Cu(II)(atsm) improve PD-like phenotypes in
87 mouse models[23–25], while other studies found improvement with treatment with a copper
88 chelator[26,27]. Furthermore, copper interacts with proteins mutated in familial forms of PD. DJ-1
89 can act as a copper chaperone to protect against metal toxicity[28,29], while copper binding to
90 alpha-synuclein promotes its aggregation[30,31]. In addition, loss of ATP7A exacerbated motor
91 phenotypes in a mouse alpha-synuclein (*SCNA*) model[32], and in *C. elegans*, PARKIN and
92 LRRK2 PD-like phenotypes were enhanced by environmental exposure to copper[33]. These data

93 suggest a strong connection between copper homeostasis and PD, however the mechanism
94 remains poorly understood.
95
96 To further explore this link between copper homeostasis and PD, we tested the functional
97 consequences of PD- or neurodegeneration associated genes that we identified as ATP7A/B
98 interactors in our previous proteomics screens[13,14] genetically interact with ATP7 using the
99 *Drosophila* model system, which we have shown recapitulates many of the phenotypes of
100 ATP7A/B human cell culture models[13,14,20,34]. We used two paradigms previously validated that
101 allow us to differentiate roles of copper homeostasis in non-neuronal cells (the epidermal
102 epithelium) and neuronal cells (dopaminergic neurons) in response to increased cellular copper
103 by ATP7 knockdown (RNAi) or copper depletion by overexpression of ATP7 in a cell
104 autonomous manner[13,20,34–37]. We find that inhibition of specific candidate genes enhances ATP7
105 knockdown phenotypes in epidermal epithelial cells in a sex dependent manner with some genes
106 showing interactions with both sexes while others only interacting in a sex-specific manner. We
107 focused on Lrrk, the fly homologue of Lrrk2 which is the most commonly mutated gene in
108 familial forms of PD and found that it genetically interacts with ATP7 in both males and females
109 in the epidermal epithelium but only in female dopaminergic neurons. These data suggest that
110 disruptions in copper homeostasis may broadly affect genes involved in PD/neurodegeneration
111 and that these interactions may contribute to disease pathology.
112
113 **Results**
114 *Coessentiality network analysis of ATP7A interactome*
115 We previously found that loss of ATP7A, a model of increased cellular copper in human cells
116 results in elevated levels of the neurodegeneration associated gene UCHL1 and that UCHL1
117 inhibition rescues ATP7 phenotypes in human cell culture and flies[38], suggesting that other
118 neurodegeneration genes in the ATP7A interactome could modulate copper-dependent
119 phenotypes as well. We first tested potential genetic interactions between ATP7A and the
120 interactome PD/neurodegeneration genes by performing a coessentiality network analysis in
121 silico (Figure S1). We assessed genome-scale fitness correlations between ATP7A with
122 ARPC1A, ARPC1B, GIGYF2, HIP1, LRKK2, VPS13C and VPS35 mining the Dependency
123 Map (DepMap) datasets[39,40]. Using the FIREWORKS tool (Fitness Interaction Rank-

124 Extrapolated netWORKs)[41], we identified that correlated and anticorrelated genes reveal
125 pathways and regulatory mechanisms connecting genes of interest with ATP7A positively (red
126 edges) and negatively (blue edges) interacting with Parkinson's and neurodegeneration genes.
127 These in silico findings support the model that ATP7A genetic interactions of similar complexity
128 may also occur in mammals as we find in *Drosophila*.
129
130 *ATP7 Genetically Interacts with Parkinson's Disease Genes*
131 We next tested if these predicted interactions from our coessentiality network analysis are
132 biological relevant using our fly ATP7 model (Table 1). In addition, we also tested two other
133 interactome candidates SCYL1 (yata in flies), a neurodegeneration associated protein which had
134 low expression levels, and the PD gene Synj1, which is a component of the endocytic pathway
135 that was identified in the interactome (Table 1)[13,14]. Knockdown of ATP7 in the fly dorsal
136 epidermal epithelium using pnr-GAL4 increases intracellular copper resulting in a decrease in
137 pigmentation in a central stipe along the back of the fly in both females and males due to
138 increased levels of intracellular copper (Figures 1B and 2B) as we and others have previously
139 observed. In addition, these flies also display a widening of the gap between the midline bristles
140 of the thorax (Figures 1B and 2B) as compared to out-crossed control pnr-GAL4 flies (Figures
141 1A and 2A). We next tested each of the ATP7A interactome genes and find that knockdown of
142 Arpc1 results in disorganized and missing midline bristles in females and males (Figures S2B
143 and S3B). Inhibition of either Gyf or yata results in missing scutellar bristles and some loss of
144 thoracic bristles (Figures S2C, J-L) in females with more mild phenotypes in males (Figures
145 S3C, J-L). Both Synj and Vps35 knockdown also leads to mild loss of scutellar bristles in
146 females and males (Figures S2E, I and S3E, I). We also observe sex differences with inhibition
147 of Hip1 and Vps13 which have no phenotype in females (Figures S2D, G-H) and mild scutellar
148 bristle loss in males (Figures S3D, G-H).
149
150 We next tested for genetic interactions between ATP7 down-regulation and inhibition of
151 these interactome genes. We find that in females, inhibition of either Arpc1, Hip1, or Vps13
152 enhances the ATP7 RNAi phenotype, resulting in a caved in thorax (Figure 1C, E, H, and Table
153 S1). In addition, the ATP7 RNAi phenotype is also enhanced in females with inhibition of yata
154 (line 1) with mild inhibition leading to increased bristle loss (Figure 1K and Table S1) and strong

155 inhibition (line 2) leading to lethality. We also observe an enhancement in disorganization of the
156 midline thoracic bristles when Vps35 was inhibited (Figure 1J and Table S1). However, not all
157 of the interactome genes interacted with ATP7 in females with neither inhibition of Gyf nor Synj
158 affecting the ATP7 down-regulation phenotype (Figure 1D, F-G and Table S1).
159
160 As ATP7 is on the X chromosome, males may be more sensitive to genetic perturbations
161 than females, and we find that similar to females Arpc1, Hip1, and Vps13 inhibition enhances
162 the ATP7 thorax caving in phenotype (Figure 2C, E, H and Table S1), though the effect of Arpc1
163 is not as strong as in females (Figure 2C vs 1C and Table S1). In addition, we find that mild
164 inhibition of yata (line 1) leads to a more severe enhancement of the ATP7 down-regulation
165 phenotype in males as compared to females (Figures 2K vs 1K and Table S1). Though Vps35
166 inhibition enhanced the ATP7 knockdown phenotype in females, we find no interaction in males
167 (Figure 2J and Table S1). In addition, unlike in females, inhibition of Synj (line 1) also leads to
168 enhancement of the phenotype (Figure 2F and Table S1), whereas similar to females Gyf
169 inhibition does not interact with ATP7 down-regulation in males (Figure 2D and Table S1).
170 These data suggest that normal expression of PD/neurodegeneration genes play a role in
171 protecting cells from increased intracellular copper and that males are more sensitive to these
172 perturbations.
173
174 *Inhibition of Lrrk enhances ATP7 down-regulation epidermal epithelium phenotypes*
175 Lrrk2 is the most commonly mutated gene in familial forms of PD[42] and regulates vesicular
176 trafficking, autophagy, and lysosomal function within cells[17,43–45]. Therefore, we next tested if
177 the Lrrk2 Drosophila orthologue, Lrrk, also plays a role in copper homeostasis using three
178 different RNAi lines (Table S2). We find that in both females and males, knockdown of Lrrk
179 alone does not affect the epidermal epithelium (Figures 3A-D, 4A-D, and Table S1). However,
180 when combined with down-regulation of ATP7, inhibition of Lrrk robustly enhanced the ATP7
181 RNAi thorax phenotype, yet to a different extent across lines (Figures 3F-H, 4F-H, and Table
182 S1). Knockdown of Lrrk results in a more severe phenotype than in males than in females. For
183 line 1, some males present with necrosis of the scutellum (Figure 4F') and line 2 displayed a
184 more pronounced caving of the thorax (Figure 4G). In addition, we find that line 3 presented
185 with mild phenotypes in females (Figure 3H and Table S1), whereas males had a more

186 pronounced phenotype with increased thoracic caving (Figure 4H and Table S1) though these
187 phenotypes were milder than line 2 (Figure 4G and Table S1). These data suggest that Lrrk acts
188 to protect epidermal epithelial cells from high levels of intracellular copper and is a more potent
189 interactor in males.
190
191 *Lrrk and ATP7 down-regulation do not interact to regulate viability*
192 As inhibiting Lrrk leads to a worsening of the ATP7 down-regulation thorax phenotypes, we
193 tested if this alters organismal viability. Though down-regulation of ATP7 does not affect
194 viability in either females or males (Figure S4A, D and Table S3), Lrrk inhibition results in
195 reduced viability (Figure S4B-C, E-F and Table S3). Furthermore, inhibiting Lrrk in the ATP7
196 down-regulation background reduces viability as compared to ATP7 knockdown alone, though
197 this is not significantly different from Lrrk inhibition alone (Figure S4B-C, E-F and Table S3).
198 These data show that the epithelial damage induced by disruption of the Lrrk and ATP7
199 interaction spares animal viability.
200
201 *Inhibition of Lrrk rescues ATP7 down-regulation dopaminergic neuronal phenotypes in a sex*
202 *dependent manner*
203 We have previously found that altering copper homeostasis in dopaminergic neurons, which are
204 lost in PD, decreases survival to a copper challenge[13,14]. Therefore, we tested whether Lrrk
205 affects these outcomes. We find that in both females and males, inhibition of either ATP7 or Lrrk
206 alone or in combination does not affect survival on glucose only food (Table S4). Knockdown of
207 ATP7 decreases survival in females when exposed to copper, whereas knockdown of Lrrk did
208 not affect survival as compared to the GAL4 control line (Figure 5A-C, Table S5). However,
209 inhibiting Lrrk in the ATP7 knockdown background, rescued survival (Figure 5A-C, Table S5).
210 In contrast, males died faster when exposed to copper and had decreased survival when either
211 ATP7 or Lrrk is inhibited (Figure 5D-F, Table S5). Knocking down Lrrk in the ATP7 down-
212 regulation background did not significantly alter survival as compared to Lrrk or ATP7 down-
213 regulation (Figure 5D-F, Table S5). These data show that Lrrk contributes to the toxicity caused
214 by increased intracellular copper in females but not males.
215
216 *Inhibition of Lrrk enhances ATP7 over-expression epidermal epithelium phenotypes*

217 In humans, both increased intracellular copper and decreased intracellular copper lead to
218 neurological disorders, therefore, we tested if inhibition of Lrrk also interacts with decreased
219 copper levels modelled by over-expression of ATP7. As we and others have previously reported,
220 over-expression of ATP7 in the epidermal epithelium results in decreased pigmentation and
221 bristle loss in both males and females (Figures 3I and 4I and[9,20,34–38]). When we combine
222 inhibition of Lrrk with over-expression of ATP7, we find increased caving in of the thorax
223 (Figures 3J-L, 4J-L, and Table S1) and in some instances a darkening of the thorax (Figure 3L
224 and Figure 4K') that is indicative of underlying internal necrosis[46,47]. Therefore, inhibition of
225 Lrrk further enhances intracellular copper depletion thorax phenotypes in both females and
226 males. Taken together, our data suggest that Lrrk normally acts to protect against both
227 accumulation (Figures 3E-H, 4E-H, and Table S1) and depletion of intracellular copper (Figures
228 3I-L, 4I-L, and Table S1).
229
230 *Inhibition of Lrrk reduces viability of ATP7 over-expression*
231 We next tested if Lrrk interacts with copper depletion for organismal viability and find that
232 similar to ATP7 down-regulation, over-expression of ATP7 does not affect viability (Figure 6
233 and Table S6). However, inhibition of Lrrk in the ATP7 over-expression background reduces
234 viability in females and males (Figure 6B-C, E-F and Table S6) but only leads to a more severe
235 reduction as compared to Lrrk inhibition alone in females (Figure 6A-C and Table S6). These
236 data indicate that in females, Lrrk acts to protect epidermal epithelial cells from copper depletion
237 but not accumulation toxicity during development to promote survival to adulthood.
238
239 *Inhibition of Lrrk in dopaminergic neurons reduces survival of ATP7 over-expression in*
240 *response to environmental copper exposure*
241 As copper depletion in the brain leads to neurological disorders, we next tested if Lrrk interacts
242 with ATP7 over-expression in dopaminergic neurons. In females, over-expression of ATP7 leads
243 to decreased survival, which is not affected by inhibition of Lrrk (Figure 7A-C, Table S7).
244 However, in males ATP7 over-expression had no effect on survival in response to copper
245 exposure though inhibition of Lrrk resulted in decreased survival (Figure 7D-F, Table S7). In
246 addition, Lrrk inhibition in the ATP7 over-expression background also led to decreased survival
247 to levels similar to Lrrk inhibition alone (Figure 7D-F, Table S7), suggesting that inhibition of

248 Lrrk does not sensitize the cell to copper depletion. Therefore, Lrrk does not interact with ATP7
249 over-expression in dopaminergic neurons in response to environmental copper exposure.
250
251 **Discussion**
252 *Copper homeostasis and PD*
253 Copper dysregulation and PD share many key features including increased oxidative stress,
254 protein aggregation, and mitochondrial damage[21,22]. In addition, PD has been associated with
255 disruptions in copper homeostasis and copper-associated toxicity[21] with PD associated genes
256 intersecting with signaling pathways that regulate metal homeostasis and counteract oxidative
257 stress[44]. We have previously performed proteomic analyses to identify interactors of the copper
258 transporter ATP7A and identified a number of genes associated with PD and/or
259 neurodegeneration[13,14]. We further confirmed a genetic interaction between ATP7A and one of
260 these candidate genes, UCHL1, which is elevated in ATP7A mutant fibroblasts and inhibition of
261 UCHL1 rescued ATP7A phenotypes[14] and may be a potential target for the development of new
262 therapeutics. Here, we have further explored how wide-spread this relationship is by testing for
263 genetic interactions between ATP7 and other candidate genes from the ATP7A interactome[13,14].
264
265 We find that a subset (7 out of the 8 genes tested) genetically interact with ATP7 and
266 play a role in protecting epidermal epithelial cells from increased intracellular copper. Five of
267 these genes (Lrrk, Hip1, Synj, Vps13, and Vps35) are associated with PD, while Arpc1 (ARPC1)
268 interacts with known PD genes[48–51]. Two common themes emerge about the functions of those
269 genes that interacted with ATP7: 1) a role in mitochondrial function/health (Vps13, Vps35, and
270 Arpc1)[44,49,50,52–56] and 2) a role in endocytosis and Golgi trafficking (Vps13, Vps35, Arpc1, yata
271 and Hip1)[4,54,57–60]. In mammalian cell culture, VPS13C plays a role in ER-late
272 endosomes/lysosome communication[57] and localizes to the outer mitochondrial membrane[53]
273 where it may also mediate communication between the mitochondria and the ER/endosomal
274 system. Vps13 (VPS13C in mammals) also leads to mitochondrial dysfunction and damage and
275 plays a role in parkin/PINK1 mediated mitophagy[53]. Similarly, a mouse model of VPS35
276 recapitulated many PD phenotypes including mitochondrial dysfunction and damage[54] and
277 impaired mitophagy in SH-SY5Y cells[55]. Interestingly both VPS13C and VPS35 play a role in
278 iron homeostasis[61,62], along with our findings, these data suggest that these genes may play a role

279 in responding to metal dyshomeostasis. Arpc1 regulates actin polymerization and plays a role in
280 a variety of cellular processes including the endosomal trafficking[59]. Upon mitochondrial
281 damage, actin filaments are assembled by Arp2/3 around the damaged mitochondria and
282 inhibition of Arp2/3 impacts mitochondrial fusion[63] and parkin mediated mitophagy[56]. In
283 addition Arp2/3 is required for the function of the retromer complex, which includes VPS35[51],
284 suggesting that the nexus between mitochondrial and endosomal-lysosomal processes may be a
285 key target for the copper induced toxicity and PD.
286
287 Though HIP1 and yata have no known mitochondrial functions, they also play a role in
288 endocytosis and endosomal trafficking. HIP1 regulates clathrin-mediated endocytosis[60] and
289 trafficking of oxidative stress responsive cell receptors[64], and Hip1 loss of function has been
290 implicated in Huntington's disease, a neurodegenerative disorder in which oxidative stress and
291 mitochondrial dysfunction are prominent pathogenic features[65], suggesting that HIP1-dependent
292 trafficking may have downstream effects on mitochondrial homeostasis. yata (SCYL1 in
293 mammals) is associated with several neurodegenerative diseases and is an accessory factor for
294 the components of coatomer I (COPI) complex to regulate trafficking between the Golgi and
295 ER[58]. Inhibition of yata in both mice and flies leads to neurodegeneration[66,67] and interacts with
296 other proteins associated with neurodegenerative diseases such as APPL (Amyloid Precursor
297 Protein-like) in flies[66] and TDP-43 in mice[68]. We have previously found that ATP7 interacts with
298 the conserved oligomeric Golgi (COG) complex, a Golgi apparatus vesicular tether[20]. This
299 connection between intracellular trafficking and copper homeostasis suggests that when these
300 trafficking genes are disrupted it could exacerbate copper toxicity by impairing copper
301 sequestration, exocytosis, or recycling or metal binding proteins.
302
303 *Sex differences in response to copper dysregulation*
304 PD and other neurological disorders can present with skewed sex ratios. For example, men are
305 1.5 times more likely to develop PD than women[69,70]. In addition, as ATP7A is a sex-linked
306 gene, Menkes disease primarily affects males[71]. Similarly, we find sex-dependent interactions
307 among these genes with Synj interacting with ATP7 in males but not females. We also observed
308 differences in severity of phenotypes across sexes as Arpc1 has milder phenotypes in males than
309 females while yata and Lrrk have more severe phenotypes in males than in females. These data

310 suggest that males and females may have different protective mechanisms against copper
311 dysregulation that intersect with some PD-associated genes but not others.
312
313 *Lrrk and ATP7 interactions are context dependent*
314 Lrrk is a kinase that regulates diverse intracellular processes, such as: mitophagy, innate
315 immunity, vesicular transport, and autophagy[17,44,45], pathways that are frequently disrupted
316 during metal-induced stress, including copper toxicity[20,72–76].
317
318 We find that the interaction between Lrrk and ATP7 are dependent on the context. For example,
319 we find that Lrrk protects against both increased and depleted levels of intracellular copper in
320 epidermal epithelial cells to maintain thoracic structure in both sexes. However, in response to
321 increased copper, males are more severely affected when Lrrk is inhibited. Furthermore, only in
322 females and only during intracellular copper depletion in the epidermal epithelium does Lrrk act
323 to promote organismal viability. These interactions are also cell type specific as we find that
324 inhibition of Lrrk in females, but not males, improved survival in response to increased levels of
325 intracellular copper (ATP7 down-regulation with copper exposure) but had no effect on survival
326 in response to depletion of intracellular copper (ATP7 over-expression with copper exposure).
327 These data suggest that Lrrk contributes to intracellular copper toxicity, and since it plays a role
328 in stress response pathways[17], Lrrk2 may help buffer cells against copper-induced toxicity.
329 Additionally, as the pathogenic G2019S mutation in Lrrk is a gain of function mutation[77,78],
330 disruptions in copper homeostasis could lead to an earlier age of onset or more severe
331 symptoms/faster disease progression.
332
333 Through this study, we have confirmed that the ATP7A interactome identified from
334 human cell culture and patient samples[13,38], represent biologically significant interactions that
335 contribute to how cells respond to disruptions in cellular homeostasis. In addition, we also find
336 that there is an intimate and common connection between copper homeostasis and genetic forms
337 of PD, which may also provide new insights into how environmental exposure to copper and
338 other heavy metals contribute to sporadic forms of PD.
339
340 **Materials and Methods**

341 *Coessentiality Analysis*

342 Coessentiality Analysis was performed with the FIREWORKS engine[41] using ATP7A with
343 ARPC1A, ARPC1B, GIGYF2, HIP1, LRKK2, VPS13C and VPS35 genes as entries in the Pan-
344 Cancer dataset as Context. The engine was run with the top 5 primary nodes and the top five
345 secondary nodes positively and negatively correlated.

346

347 *Drosophila Strains and Husbandry*

348 The following strains were obtained from the Bloomington *Drosophila* Stock Center,
349 Bloomington, IL: w1118 (#5905), Ddc-Gal4 (#7009), pnr-Gal4 (#3039), UAS-Lrrk-RNAi-1
350 (#32457), UAS-Lrrk-RNAi-2 (#39019), and UAS-Lrrk-RNAi-3 (#35249). The UAS-ATP7-
351 RNAi (#108159) stock was obtained from the Vienna *Drosophila* Resource Center. The UAS-
352 ATP7-wt (overexpression) was a gift from Richard Burke, Monash University, Australia. See
353 Table S2 for a full list of genotypes. All stocks were reared on standard Molasses Food (Genesee
354 Scientific) at 25°C in 12hr:12hr light:dark cycle.

355

356 *Imaging*

357 ATP7A interactome candidate genes were knocked down in epidermal epithelium cells in either
358 an ATP7 loss of function or overexpression background using the pnr-Gal4 driver. 1-week-old
359 flies were imaged using a LEICA S6D stereomicroscope with a Leica EC4 Digital Camera. Z-
360 stacks were then aligned and max projections generated using Zerene Stacker.

361

362 *Viability Assay*

363 Three biological replicates of 8-10 virgin females were crossed with 4-5 males for each
364 genotype. The flies were transferred into new vials every three days resulting in three technical
365 replicates for each cross. Once the offspring began eclosing, they were tracked for nine days,
366 accounting for the number of males and females for each expected genotype were recorded. All
367 crosses were reared on standard Molasses Food (Genesee Scientific) at 25°C in 12hr:12hr
368 light:dark cycle.

369

370 *Copper Toxicity Assay*

Copper feedings were performed on 1-week-old virgin females and males reared separately. ATP7 was either knockdown or overexpressed alone or in combination with Lrrk knockdown in the dopaminergic neurons using the Ddc-Gal4 driver. Flies were starved for 3 hours and transferred to empty vials with Whatman glass microfiber filter discs saturated in either 1 mM $CuSO_4$ + 5% glucose solution or 5% glucose solution. Survival was assayed for every 12-24 hours for five days. Experiments were performed with a minimum of 10 replicates per genotype per sex with ~10 flies per replicate at 25°C in 12hr:12hr light:dark cycle.

Statistical Analysis

The results of the copper toxicity assay were tested for statistical significance testing survival and proportion data. Survival data was tested using Kaplan-Meier survival analysis, log-rank tests, and pairwise comparisons to assess the significance between genotypes and survival time. Proportion data for copper survival and viability were tested by creating a generalized linear model and an analysis of deviance table was used to fit variance using chi-squared tests for significance, per-time contrasts were conducted with post emmeans testing with tukey adjustment. All statistical analyses were performed in R.

Acknowledgements

We would also like to acknowledge the Bloomington Drosophila Stock Center (NIH P40OD018537), and the Vienna Drosophila Resource Center for providing fly stocks used in this study. Funding for this project included start-up funds from Illinois State University and Oregon State University, and R15AR070505 to AVM, and 1RF1AG060285 to VF. EW is supported by NIH grant ES034796 and NG is supported by 1T32GM160704-01. The content is solely the responsibility of the authors and does not necessarily represent the official views of the National Institutes of Health. The funders had no role in study design, data collection and analysis, decision to publish, or preparation of the manuscript.

Author Contributions

BA and NG performed experiments and data analysis. EW, VF, and AVM made intellectual contributions to experimental design, data analysis and interpretation, and provided funding. All authors were involved in reading and editing the manuscript.

402

403 **Conflict of Interest Statement**

404 The authors have no conflicts of interest.

405

406 **Data Availability Statement**

407 The data that support the findings of this study are available from the corresponding author upon
408 reasonable request.

409

410 **References**

411 1. Henriksen, C., and Arnesen, E.K. (2023). Copper – a scoping review for Nordic Nutrition
412 Recommendations 2023. Food Nutr. Res. *67*, 10.29219/fnr.v67.10322.
413 https://doi.org/10.29219/fnr.v67.10322.

414 2. An, Y., Li, S., Huang, X., Chen, X., Shan, H., and Zhang, M. (2022). The Role of Copper
415 Homeostasis in Brain Disease. Int. J. Mol. Sci. *23*, 13850.
416 https://doi.org/10.3390/ijms232213850.

417 3. EFSA Panel on Dietetic Products, Nutrition and Allergies (NDA) (2015). Scientific Opinion
418 on Dietary Reference Values for copper. EFSA J. *13*, 4253.
419 https://doi.org/10.2903/j.efsa.2015.4253.

420 4. Lutsenko, S., Bhattacharjee, A., and Hubbard, A.L. (2010). Copper handling machinery of
421 the brain. Met. Integr. Biometal Sci. *2*, 596–608. https://doi.org/10.1039/c0mt00006j.

422 5. Lutsenko, S., Barnes, N.L., Bartee, M.Y., and Dmitriev, O.Y. (2007). Function and
423 Regulation of Human Copper-Transporting ATPases. Physiol. Rev. *87*, 1011–1046.
424 https://doi.org/10.1152/physrev.00004.2006.

425 6. Chen, L., Min, J., and Wang, F. (2022). Copper homeostasis and cuproptosis in health and
426 disease. Signal Transduct. Target. Ther. *7*, 378. https://doi.org/10.1038/s41392-022-01229-y.

427 7. Lane, A.R., Roberts, B.R., Fahrni, C.J., and Faundez, V. (2025). A primer on copper biology
428 in the brain. Neurobiol. Dis. *212*, 106974. https://doi.org/10.1016/j.nbd.2025.106974.

429 8. Zlatic, S., Comstra, H.S., Gokhale, A., Petris, M.J., and Faundez, V. (2015). Molecular Basis
430 of Neurodegeneration and Neurodevelopmental Defects in Menkes Disease. Neurobiol. Dis.
431 *81*, 154–161. https://doi.org/10.1016/j.nbd.2014.12.024.

432 9. Hartwig, C., Zlatic, S.A., Wallin, M., Vrailas-Mortimer, A., Fahrni, C.J., and Faundez, V.
433 (2019). Trafficking mechanisms of P-type ATPase copper transporters. Curr. Opin. Cell
434 Biol. *59*, 24–33. https://doi.org/10.1016/j.ceb.2019.02.009.

435 10. Kaler, S.G. (2011). ATP7A-related copper transport diseases—emerging concepts and future
436 trends. Nat. Rev. Neurol. *7*, 15–29. https://doi.org/10.1038/nrneurol.2010.180.

437 11. Tümer, Z., and Møller, L.B. (2010). Menkes disease. Eur. J. Hum. Genet. *18*, 511–518.
438 https://doi.org/10.1038/ejhg.2009.187.

439 12. Hwang, J.E.C., de Bruyne, M., Warr, C.G., and Burke, R. (2014). Copper overload and
440 deficiency both adversely affect the central nervous system of Drosophila. Met. Integr.
441 Biometal Sci. *6*, 2223–2229. https://doi.org/10.1039/c4mt00140k.

442 13. Comstra, H.S., McArthy, J., Rudin-Rush, S., Hartwig, C., Gokhale, A., Zlatic, S.A.,
443 Blackburn, J.B., Werner, E., Petris, M., D'Souza, P., et al. (2017). The interactome of the
444 copper transporter ATP7A belongs to a network of neurodevelopmental and
445 neurodegeneration factors. eLife *6*, e24722. https://doi.org/10.7554/eLife.24722.

446 14. Zlatic, S.A., Vrailas-Mortimer, A., Gokhale, A., Carey, L.J., Scott, E., Burch, R., McCall,
447 M.M., Rudin-Rush, S., Davis, J.B., Hartwig, C., et al. (2018). Rare Disease Mechanisms
448 Identified by Genealogical Proteomics of Copper Homeostasis Mutant Pedigrees. Cell Syst.
449 *6*, 368-380.e6. https://doi.org/10.1016/j.cels.2018.01.008.

450 15. Tysnes, O.-B., and Storstein, A. (2017). Epidemiology of Parkinson's disease. J. Neural
451 Transm. *124*, 901–905. https://doi.org/10.1007/s00702-017-1686-y.

452 16. Pringsheim, T., Jette, N., Frolkis, A., and Steeves, T.D.L. (2014). The prevalence of
453 Parkinson's disease: A systematic review and meta-analysis. Mov. Disord. *29*, 1583–1590.
454 https://doi.org/10.1002/mds.25945.

455 17. Klein, C., and Westenberger, A. (2012). Genetics of Parkinson's Disease. Cold Spring Harb.
456 Perspect. Med. *2*, a008888. https://doi.org/10.1101/cshperspect.a008888.

457 18. Alvarez-Vega, R., Rios, C., Rojas, P., and Kravsov, J. (1992). MPTP treatment decreases
458 striatal copper content in mice. Proc. West. Pharmacol. Soc. *35*, 25–27.

459 19. Matusch, A., Depboylu, C., Palm, C., Wu, B., Höglinger, G.U., Schäfer, M.K.-H., and
460 Becker, J.S. (2010). Cerebral bioimaging of Cu, Fe, Zn, and Mn in the MPTP mouse model
461 of Parkinson's disease using laser ablation inductively coupled plasma mass spectrometry
462 (LA-ICP-MS). J. Am. Soc. Mass Spectrom. *21*, 161–171.
463 https://doi.org/10.1016/j.jasms.2009.09.022.

464 20. Hartwig, C., Méndez, G.M., Bhattacharjee, S., Vrailas-Mortimer, A.D., Zlatic, S.A.,
465 Freeman, A.A.H., Gokhale, A., Concilli, M., Werner, E., Sapp Savas, C., et al. (2021).
466 Golgi-Dependent Copper Homeostasis Sustains Synaptic Development and Mitochondrial
467 Content. J. Neurosci. Off. J. Soc. Neurosci. *41*, 215–233.
468 https://doi.org/10.1523/JNEUROSCI.1284-20.2020.

469 21. Bisaglia, M., and Bubacco, L. (2020). Copper Ions and Parkinson's Disease: Why Is
470 Homeostasis So Relevant? Biomolecules *10*, 195. https://doi.org/10.3390/biom10020195.

22. Davies, K.M., Bohic, S., Carmona, A., Ortega, R., Cottam, V., Hare, D.J., Finberg, J.P.M., Reyes, S., Halliday, G.M., Mercer, J.F.B., et al. (2014). Copper pathology in vulnerable brain regions in Parkinson's disease. Neurobiol. Aging *35*, 858–866. https://doi.org/10.1016/j.neurobiolaging.2013.09.034.

23. Hung, L.W., Villemagne, V.L., Cheng, L., Sherratt, N.A., Ayton, S., White, A.R., Crouch, P.J., Lim, S., Leong, S.L., Wilkins, S., et al. (2012). The hypoxia imaging agent CuII(atsm) is neuroprotective and improves motor and cognitive functions in multiple animal models of Parkinson's disease. J. Exp. Med. *209*, 837–854. https://doi.org/10.1084/jem.20112285.

24. Cheng, Y., Wang, G., Yang, X., Wang, Y., Li, D., Zhao, Y., and Zhang, F. (2025). Artesunate alleviates Parkinson's disease by targeting astrocyte MT2A to attenuate dopamine neuronal cuproptosis. Pharmacol. Res. *219*, 107895. https://doi.org/10.1016/j.phrs.2025.107895.

25. Alcaraz-Zubeldia, M., Rojas, P., Boll, C., and Ríos, C. (2001). Neuroprotective Effect of Acute and Chronic Administration of Copper (II) Sulfate against MPP+ Neurotoxicity in Mice. Neurochem. Res. *26*, 59–64. https://doi.org/10.1023/A:1007680616056.

26. Aguirre, P., García-Beltrán, O., Tapia, V., Muñoz, Y., Cassels, B.K., and Núñez, M.T. (2017). Neuroprotective Effect of a New 7,8-Dihydroxycoumarin-Based Fe2+/Cu2+ Chelator in Cell and Animal Models of Parkinson's Disease. ACS Chem. Neurosci. *8*, 178–185. https://doi.org/10.1021/acschemneuro.6b00309.

27. Leuci, R., Brunetti, L., Tufarelli, V., Cerini, M., Paparella, M., Puvača, N., and Piemontese, L. (2024). Role of copper chelating agents: between old applications and new perspectives in neuroscience. Neural Regen. Res. *20*, 751–762. https://doi.org/10.4103/NRR.NRR-D-24-00140.

28. Björkblom, B., Adilbayeva, A., Maple-Grødem, J., Piston, D., Ökvist, M., Xu, X.M., Brede, C., Larsen, J.P., and Møller, S.G. (2013). Parkinson disease protein DJ-1 binds metals and protects against metal-induced cytotoxicity. J. Biol. Chem. *288*, 22809–22820. https://doi.org/10.1074/jbc.M113.482091.

29. Girotto, S., Cendron, L., Bisaglia, M., Tessari, I., Mammi, S., Zanotti, G., and Bubacco, L. (2014). DJ-1 is a copper chaperone acting on SOD1 activation. J. Biol. Chem. *289*, 10887–10899. https://doi.org/10.1074/jbc.M113.535112.

30. Paik, S.R., Shin, H.J., and Lee, J.H. (2000). Metal-catalyzed oxidation of alpha-synuclein in the presence of Copper(II) and hydrogen peroxide. Arch. Biochem. Biophys. *378*, 269–277. https://doi.org/10.1006/abbi.2000.1822.

31. Walke, G., Kumar, R., and Wittung-Stafshede, P. (2024). Copper ion incorporation in α-synuclein amyloids. Protein Sci. Publ. Protein Soc. *33*, e4956. https://doi.org/10.1002/pro.4956.

507 32. Casey, M., Zou, D., Reijo Pera, R.A., Hensley-McBain, T., and Cabin, D.E. (2025). Alpha-
508 synuclein null mutation exacerbates the phenotype of a model of Menkes disease in female
509 mice. Front. Neurosci. *19*, 1613171. https://doi.org/10.3389/fnins.2025.1613171.

510 33. Weishaupt, A.-K., Ruecker, L., Meiners, T., Schwerdtle, T., Silva Avila, D., Aschner, M.,
511 and Bornhorst, J. (2024). Copper-mediated neurotoxicity and genetic vulnerability in the
512 background of neurodegenerative diseases in C. elegans. Toxicol. Sci. Off. J. Soc. Toxicol.
513 *201*, 254–262. https://doi.org/10.1093/toxsci/kfae092.

514 34. Lane, A.R., Scher, N.E., Bhattacharjee, S., Zlatic, S.A., Roberts, A.M., Gokhale, A.,
515 Singleton, K.S., Duong, D.M., McKenna, M., Liu, W.L., et al. (2025). Adaptive protein
516 synthesis in genetic models of copper deficiency and childhood neurodegeneration. Mol.
517 Biol. Cell *36*, ar33. https://doi.org/10.1091/mbc.E24-11-0512.

518 35. Hwang, J.E.C., de Bruyne, M., Warr, C.G., and Burke, R. (2014). Copper overload and
519 deficiency both adversely affect the central nervous system of Drosophila†. Metallomics *6*,
520 2223–2229. https://doi.org/10.1039/c4mt00140k.

521 36. Norgate, M., Lee, E., Southon, A., Farlow, A., Batterham, P., Camakaris, J., and Burke, R.
522 (2006). Essential roles in development and pigmentation for the Drosophila copper
523 transporter DmATP7. Mol. Biol. Cell *17*, 475–484. https://doi.org/10.1091/mbc.e05-06-
524 0492.

525 37. Burke, R., Commons, E., and Camakaris, J. (2008). Expression and localisation of the
526 essential copper transporter DmATP7 in Drosophila neuronal and intestinal tissues. Int. J.
527 Biochem. Cell Biol. *40*, 1850–1860. https://doi.org/10.1016/j.biocel.2008.01.021.

528 38. Zlatic, S.A., Vrailas-Mortimer, A., Gokhale, A., Carey, L.J., Scott, E., Burch, R., McCall,
529 M.M., Rudin-Rush, S., Davis, J.B., Hartwig, C., et al. (2018). Rare Disease Mechanisms
530 Identified by Genealogical Proteomics of Copper Homeostasis Mutant Pedigrees. Cell Syst.
531 *6*, 368-380.e6. https://doi.org/10.1016/j.cels.2018.01.008.

532 39. Arafeh, R., Shibue, T., Dempster, J.M., Hahn, W.C., and Vazquez, F. (2025). The present
533 and future of the Cancer Dependency Map. Nat. Rev. Cancer *25*, 59–73.
534 https://doi.org/10.1038/s41568-024-00763-x.

535 40. Tsherniak, A., Vazquez, F., Montgomery, P.G., Weir, B.A., Kryukov, G., Cowley, G.S., Gill,
536 S., Harrington, W.F., Pantel, S., Krill-Burger, J.M., et al. (2017). Defining a Cancer
537 Dependency Map. Cell *170*, 564-576.e16. https://doi.org/10.1016/j.cell.2017.06.010.

538 41. Amici, D.R., Jackson, J.M., Truica, M.I., Smith, R.S., Abdulkadir, S.A., and Mendillo, M.L.
539 (2021). FIREWORKS: a bottom-up approach to integrative coessentiality network analysis.
540 Life Sci. Alliance *4*. https://doi.org/10.26508/lsa.202000882.

541 42. Ravinther, A.I., Dewadas, H.D., Tong, S.R., Foo, C.N., Lin, Y.-E., Chien, C.-T., and Lim,
542 Y.M. (2022). Molecular Pathways Involved in LRRK2-Linked Parkinson's Disease: A
543 Systematic Review. Int. J. Mol. Sci. *23*, 11744. https://doi.org/10.3390/ijms231911744.

544 43. Taymans, J.-M., Fell, M., Greenamyre, T., Hirst, W.D., Mamais, A., Padmanabhan, S., Peter,
545 I., Rideout, H., and Thaler, A. (2023). Perspective on the current state of the LRRK2 field.
546 Npj Park. Dis. *9*, 104. https://doi.org/10.1038/s41531-023-00544-7.

547 44. Trinh, J., and Farrer, M. (2013). Advances in the genetics of Parkinson disease. Nat. Rev.
548 Neurol. *9*, 445–454. https://doi.org/10.1038/nrneurol.2013.132.

549 45. Sanna, G., Del Giudice, M.G., Crosio, C., and Iaccarino, C. (2012). LRRK2 and vesicle
550 trafficking. Biochem. Soc. Trans. *40*, 1117–1122. https://doi.org/10.1042/BST20120117.

551 46. Zhang, B., Binks, T., and Burke, R. (2020). The E3 ubiquitin ligase Slimb/β-TrCP is
552 required for normal copper homeostasis in *Drosophila*. Biochim. Biophys. Acta BBA - Mol.
553 Cell Res. *1867*, 118768. https://doi.org/10.1016/j.bbamcr.2020.118768.

554 47. Green, C., Levashina, E., McKimmie, C., Dafforn, T., Reichhart, J.M., and Gubb, D. (2000).
555 The necrotic gene in Drosophila corresponds to one of a cluster of three serpin transcripts
556 mapping at 43A1.2. Genetics *156*, 1117–1127. https://doi.org/10.1093/genetics/156.3.1117.

557 48. Karpenko, M.N., Muruzheva, Z.M., Ilyechova, E.Y., Babich, P.S., and Puchkova, L.V.
558 (2023). Abnormalities in Copper Status Associated with an Elevated Risk of Parkinson's
559 Phenotype Development. Antioxid. Basel Switz. *12*, 1654.
560 https://doi.org/10.3390/antiox12091654.

561 49. Kinnart, I., Manders, L., Heyninck, T., Imberechts, D., Praschberger, R., Schoovaerts, N.,
562 Verfaillie, C., Verstreken, P., and Vandenberghe, W. (2024). Elevated α-synuclein levels
563 inhibit mitophagic flux. NPJ Park. Dis. *10*, 80. https://doi.org/10.1038/s41531-024-00696-0.

564 50. Sarkar, S., Olsen, A.L., Sygnecka, K., Lohr, K.M., and Feany, M.B. (2021). α-synuclein
565 impairs autophagosome maturation through abnormal actin stabilization. PLoS Genet. *17*,
566 e1009359. https://doi.org/10.1371/journal.pgen.1009359.

567 51. Petyuk, V.A., Yu, L., Olson, H.M., Yu, F., Clair, G., Qian, W.-J., Shulman, J.M., and
568 Bennett, D.A. (2021). Proteomic Profiling of the Substantia Nigra to Identify Determinants
569 of Lewy Body Pathology and Dopaminergic Neuronal Loss. J. Proteome Res. *20*, 2266–
570 2282. https://doi.org/10.1021/acs.jproteome.0c00747.

571 52. Vidyadhara, D.J., Lee, J.E., and Chandra, S.S. (2019). Role of the Endolysosomal System in
572 Parkinson's disease. J. Neurochem. *150*, 487–506. https://doi.org/10.1111/jnc.14820.

573 53. Lesage, S., Drouet, V., Majounie, E., Deramecourt, V., Jacoupy, M., Nicolas, A., Cormier-
574 Dequaire, F., Hassoun, S.M., Pujol, C., Ciura, S., et al. (2016). Loss of VPS13C Function in
575 Autosomal-Recessive Parkinsonism Causes Mitochondrial Dysfunction and Increases
576 PINK1/Parkin-Dependent Mitophagy. Am. J. Hum. Genet. *98*, 500–513.
577 https://doi.org/10.1016/j.ajhg.2016.01.014.

578 54. Niu, M., Zhao, F., Bondelid, K., Siedlak, S.L., Torres, S., Fujioka, H., Wang, W., Liu, J., and
579 Zhu, X. (2021). VPS35 D620N knockin mice recapitulate cardinal features of Parkinson's
580 disease. Aging Cell *20*, e13347. https://doi.org/10.1111/acel.13347.

581 55. Ma, K.Y., Fokkens, M.R., Reggiori, F., Mari, M., and Verbeek, D.S. (2021). Parkinson's
582 disease-associated VPS35 mutant reduces mitochondrial membrane potential and impairs
583 PINK1/Parkin-mediated mitophagy. Transl. Neurodegener. *10*, 19.
584 https://doi.org/10.1186/s40035-021-00243-4.

585 56. Fung, T.S., Ghosh, A., Zavala, M.R., Nichtova, Z., Shukal, D., Tigano, M., Csordas, G.,
586 Higgs, H.N., and Chakrabarti, R. (2025). Peri-mitochondrial actin filaments inhibit Parkin
587 assembly by disrupting ER-mitochondria contacts. EMBO Rep., 1–32.
588 https://doi.org/10.1038/s44319-025-00561-y.

589 57. Kumar, N., Leonzino, M., Hancock-Cerutti, W., Horenkamp, F.A., Li, P., Lees, J.A.,
590 Wheeler, H., Reinisch, K.M., and De Camilli, P. (2018). VPS13A and VPS13C are lipid
591 transport proteins differentially localized at ER contact sites. J. Cell Biol. *217*, 3625–3639.
592 https://doi.org/10.1083/jcb.201807019.

593 58. Burman, J.L., Bourbonniere, L., Philie, J., Stroh, T., Dejgaard, S.Y., Presley, J.F., and
594 McPherson, P.S. (2008). Scyl1, mutated in a recessive form of spinocerebellar
595 neurodegeneration, regulates COPI-mediated retrograde traffic. J. Biol. Chem. *283*, 22774–
596 22786. https://doi.org/10.1074/jbc.M801869200.

597 59. Taunton, J., Rowning, B.A., Coughlin, M.L., Wu, M., Moon, R.T., Mitchison, T.J., and
598 Larabell, C.A. (2000). Actin-dependent propulsion of endosomes and lysosomes by
599 recruitment of N-WASP. J. Cell Biol. *148*, 519–530. https://doi.org/10.1083/jcb.148.3.519.

600 60. Buenaventura, T., Kanda, N., Douzenis, P.C., Jones, B., Bloom, S.R., Chabosseau, P.,
601 Corrêa, I.R., Bosco, D., Piemonti, L., Marchetti, P., et al. (2018). A Targeted RNAi Screen
602 Identifies Endocytic Trafficking Factors That Control GLP-1 Receptor Signaling in
603 Pancreatic β-Cells. Diabetes *67*, 385–399. https://doi.org/10.2337/db17-0639.

604 61. Xue, Y., Schmollinger, S., Attar, N., Campos, O.A., Vogelauer, M., Carey, M.F., Merchant,
605 S.S., and Kurdistani, S.K. (2017). Endoplasmic reticulum-mitochondria junction is required
606 for iron homeostasis. J. Biol. Chem. *292*, 13197–13204.
607 https://doi.org/10.1074/jbc.M117.784249.

608 62. Bórquez, D.A., Castro, F., Núñez, M.T., and Urrutia, P.J. (2022). New Players in Neuronal
609 Iron Homeostasis: Insights from CRISPRi Studies. Antioxid. Basel Switz. *11*, 1807.
610 https://doi.org/10.3390/antiox11091807.

611 63. Gatti, P., Schiavon, C., Cicero, J., Manor, U., and Germain, M. (2025). Mitochondria- and
612 ER-associated actin are required for mitochondrial fusion. Nat. Commun. *16*, 451.
613 https://doi.org/10.1038/s41467-024-55758-x.

614 64. Metzler, M., Li, B., Gan, L., Georgiou, J., Gutekunst, C.-A., Wang, Y., Torre, E., Devon,
615 R.S., Oh, R., Legendre-Guillemin, V., et al. (2003). Disruption of the endocytic protein HIP1
616 results in neurological deficits and decreased AMPA receptor trafficking. EMBO J. *22*,
617 3254–3266. https://doi.org/10.1093/emboj/cdg334.

618 65. Bhattacharyya, N.P., Banerjee, M., and Majumder, P. (2008). Huntington's disease: roles of
619 huntingtin-interacting protein 1 (HIP-1) and its molecular partner HIPPI in the regulation of
620 apoptosis and transcription. FEBS J. *275*, 4271–4279. https://doi.org/10.1111/j.1742-
621 4658.2008.06563.x.

622 66. Sone, M., Uchida, A., Komatsu, A., Suzuki, E., Ibuki, I., Asada, M., Shiwaku, H., Tamura,
623 T., Hoshino, M., Okazawa, H., et al. (2009). Loss of yata, a novel gene regulating the
624 subcellular localization of APPL, induces deterioration of neural tissues and lifespan
625 shortening. PloS One *4*, e4466. https://doi.org/10.1371/journal.pone.0004466.

626 67. Schmidt, W.M., Kraus, C., Höger, H., Hochmeister, S., Oberndorfer, F., Branka, M.,
627 Bingemann, S., Lassmann, H., Müller, M., Macedo-Souza, L.I., et al. (2007). Mutation in the
628 Scyl1 gene encoding amino-terminal kinase-like protein causes a recessive form of
629 spinocerebellar neurodegeneration. EMBO Rep. *8*, 691–697.
630 https://doi.org/10.1038/sj.embor.7401001.

631 68. Pelletier, S., Gingras, S., Howell, S., Vogel, P., and Ihle, J.N. (2012). An early onset
632 progressive motor neuron disorder in Scyl1-deficient mice is associated with mislocalization
633 of TDP-43. J. Neurosci. Off. J. Soc. Neurosci. *32*, 16560–16573.
634 https://doi.org/10.1523/JNEUROSCI.1787-12.2012.

635 69. Cerri, S., Mus, L., and Blandini, F. Parkinson's Disease in Women and Men: What's the
636 Difference? J. Park. Dis. *9*, 501–515. https://doi.org/10.3233/JPD-191683.

637 70. Moisan, F., Kab, S., Mohamed, F., Canonico, M., Guern, M.L., Quintin, C., Carcaillon, L.,
638 Nicolau, J., Duport, N., Singh-Manoux, A., et al. (2016). Parkinson disease male-to-female
639 ratios increase with age: French nationwide study and meta-analysis. J. Neurol. Neurosurg.
640 Psychiatry *87*, 952–957. https://doi.org/10.1136/jnnp-2015-312283.

641 71. Tümer, Z., and Møller, L.B. (2010). Menkes disease. Eur. J. Hum. Genet. *18*, 511–518.
642 https://doi.org/10.1038/ejhg.2009.187.

643 72. Aschner, M., Skalny, A.V., Lu, R., Martins, A.C., Tizabi, Y., Nekhoroshev, S.V.,
644 Santamaria, A., Sinitskiy, A.I., and Tinkov, A.A. (2024). Mitochondrial pathways of copper
645 neurotoxicity: focus on mitochondrial dynamics and mitophagy. Front. Mol. Neurosci. *17*,
646 1504802. https://doi.org/10.3389/fnmol.2024.1504802.

647 73. Lu, J., Liu, X., Li, X., Li, H., Shi, L., Xia, X., He, B.-L., Meyer, T.F., Li, X., Sun, H., et al.
648 (2024). Copper regulates the host innate immune response against bacterial infection via
649 activation of ALPK1 kinase. Proc. Natl. Acad. Sci. U. S. A. *121*, e2311630121.
650 https://doi.org/10.1073/pnas.2311630121.

651 74. O'Sullivan, E., O'Shea, D., Devereux, M., Kavanagh, K., and Howe, O. (2026). Autophagy-
652 dependent cell death and immune responses induced by heteroleptic copper(II),
653 manganese(II), and silver(I) complexes containing dicarboxylate and 1,10-phenanthroline
654 ligands: novel insights from in vitro and in vivo models. Biometals Int. J. Role Met. Ions
655 Biol. Biochem. Med. *39*, 337–358. https://doi.org/10.1007/s10534-025-00766-7.

656 75. Duncan, C., Bica, L., Crouch, P.J., Caragounis, A., Lidgerwood, G.E., Parker, S.J.,
657 Meyerowitz, J., Volitakis, I., Liddell, J.R., Raghupathi, R., et al. (2013). Copper modulates
658 the large dense core vesicle secretory pathway in PC12 cells. Met. Integr. Biometal Sci. *5*,
659 700–714. https://doi.org/10.1039/c3mt20231c.

660 76. Seo, Y., Cho, Y.-S., Huh, Y.-D., and Park, H. (2016). Copper Ion from Cu2O Crystal
661 Induces AMPK-Mediated Autophagy via Superoxide in Endothelial Cells. Mol. Cells *39*,
662 195–203. https://doi.org/10.14348/molcells.2016.2198.

663 77. Lee, B.D., Shin, J.-H., VanKampen, J., Petrucelli, L., West, A.B., Ko, H.S., Lee, Y.-I.,
664 Maguire-Zeiss, K.A., Bowers, W.J., Federoff, H.J., et al. (2010). Inhibitors of leucine-rich
665 repeat kinase-2 protect against models of Parkinson's disease. Nat. Med. *16*, 998–1000.
666 https://doi.org/10.1038/nm.2199.

667 78. Liu, Z., Wang, X., Yu, Y., Li, X., Wang, T., Jiang, H., Ren, Q., Jiao, Y., Sawa, A., Moran,
668 T., et al. (2008). A Drosophila model for LRRK2-linked parkinsonism. Proc. Natl. Acad. Sci.
669 U. S. A. *105*, 2693–2698. https://doi.org/10.1073/pnas.0708452105.

670

671

672

673

674 **Figure Legends**

675

676 **Figure 1. ATP7 Interacts with Parkinson's Disease/Neurodegeneration Genes in the**
677 **Epidermal Epithelium in Females.** Images of inhibition of ATP7 alone **A)** or in combination
678 with inhibition of different ATP7 interactome homologues using the pnr-GAL4 in females **B-L).**
679 Yellow arrows indicate widening of the thoracic midline bristles, red arrows indicate areas of
680 thoracic caving in, black arrows show scutellar bristle defects, and yellow arrowhead indicates
681 bristle disorganization.

682

683 **Figure 2. ATP7 Interacts with Parkinson's Disease/Neurodegeneration Genes in the**
684 **Epidermal Epithelium in Males.** Images of inhibition of ATP7 alone **A)** or in combination with
685 inhibition of different ATP7 interactome homologues using the pnr-GAL4 in males **B-L).**
686 Yellow arrows indicate areas of thoracic caving in, and red arrows indicate areas of thoracic
687 caving in, black arrows show scutellar bristle defects, and yellow arrowhead indicates missing
688 and disorganized thoracic bristles.

689

690 **Figure 3. ATP7 Interacts with Lrrk in the Epidermal Epithelium in Females.** Images of
691 control **A)** and different Lrrk RNAi lines **B-D)** using the pnr-GAL4 in females**.** ATP7 down-
692 regulation alone **E)** or in combination with inhibition of Lrrk **F-H).** ATP7 over-expression **I)**
693 alone or in combination with inhibition of Lrrk **J-L)**. Yellow arrows indicate widening of the
694 bristles along the midline of the thorax. Red arrows indicate thoracic caving in, and yellow
695 arrowheads indicate bristle loss.

696

697 **Figure 4. ATP7 Interacts with Lrrk in the Epidermal Epithelium in Males.** Images of
698 control **A)** and different Lrrk RNAi lines **B-D)** using the pnr-GAL4 in males**.** ATP7 down-
699 regulation alone **E)** or in combination with inhibition of Lrrk **F-H).** ATP7 over-expression **I)**
700 alone or in combination with inhibition of Lrrk **J-L)**. Red arrows indicate thoracic caving in, and
701 black arrowheads indicate necrotic tissue.

702

703 **Figure 5. Lrrk Interacts with ATP7 Down-regulation and Copper Exposure in**
704 **Dopaminergic Neurons.** Female **A-C)** and male **D-F)** flies exposed to copper with either
705 inhibition of ATP7 alone or in combination with Lrrk inhibition using the Ddc-GAL4.

706

707 **Figure 6. Lrrk Interacts with ATP7 Over-expression and Viability.** The normalized ratio of
708 female **A-C)** and male **D-F)** flies that were expected to reach adulthood (viability) with either
709 down-regulation of ATP7 alone or in combination with Lrrk inhibition using the Ddc-GAL4. For
710 Lrrk RNAi line 1 females, statistical results $\chi^2 = 10.93$, df = 3, p-value = 0.01211. For Lrrk
711 RNAi line 2 females, statistical results $\chi^2 = 120.44$, df = 3, p-value < 2.2e-16. For Lrrk RNAi
712 line 3 females, statistical results $\chi^2 = 41.642$, df = 3, p-value = 4.778e-09. For Lrrk RNAi line 1
713 males, statistical results $\chi^2 = 12.034$, df = 3, p-value = 0.007268. For Lrrk RNAi line 2 males,
714 statistical results $\chi^2 = 141.32$, df = 3, p-value < 2.2e-16. For Lrrk RNAi line 3 females, statistical
715 results $\chi^2 = 31.117$, df = 3, p-value = 8.03e-07.

716

717 **Figure 7. Lrrk Interacts with ATP7 Over-expression and Copper Exposure in**
718 **Dopaminergic Neurons.** Female **A-C)** and male **D-F)** flies exposed to copper with either over-
719 expression of ATP7 alone or in combination with Lrrk inhibition using the Ddc-GAL4.

720

721 **Figure S1. Coessentiality Network Analysis of ATP7A.**

722 Coessentiality network analysis showing genome-scale fitness correlations of ATP7A and
723 Parkinson's and neurodegeneration genes as inputs. Nodes correspond to first and second level
724 interaction nodes. Network of correlated (red edges) and anticorrelated genes (blue edges) was
725 built with the FIREWORKS tool.

726

727 **Figure S2. Inhibition of Lrrk in the Epidermal Epithelium in Females.** Images of inhibition
728 of ATP7 interactome genes using the pnr-GAL4 in females. Yellow arrows indicate missing and
729 disorganization thoracic midline bristles. Black arrows show loss of scutellar bristles.

730

731 **Figure S3. Inhibition of Lrrk in the Epidermal Epithelium in Males.** Images of inhibition of
732 ATP7 interactome genes using the pnr-GAL4 in females. Yellow arrows indicate missing and
733 disorganization thoracic midline bristles. Black arrows show loss of scutellar bristles.

734

735 **Figure S4. Lrrk Interacts with ATP7 Down-regulation and Viability.** The normalized ratio of
736 female **A-C) and** male **D-F)** flies that were expected to reach adulthood (viability) with either
737 down-regulation of ATP7 alone or in combination with Lrrk inhibition using the Ddc-GAL4. For
738 Lrrk RNAi line 1 females, statistical results $\chi^2 = 7.1566$, df = 3, p-value = 0.06707. For Lrrk
739 RNAi line 2 females, statistical results $\chi^2 = 112.05$, df = 3, p-value < 2.2e-16. For Lrrk RNAi
740 line 3 females, statistical results $\chi^2 = 47.872$, df = 3, p-value = 2.267e-10. For Lrrk RNAi line 1
741 males, statistical results $\chi^2 = 6.052$, df = 3, p-value = 0.1091. For Lrrk RNAi line 2 males,
742 statistical results $\chi^2 = 97.556$, df = 3, p-value < 2.2e-16. For Lrrk RNAi line 3 females, statistical
743 results $\chi^2 = 64.697$, df = 3, p-value = 5.823e-14.

744

745 **Table 1. *Drosophila* Homologues of ATP7A Interactome Genes**
746

747 **Table S1. Summary of Interactions Between ATP7 Down-regulation and Interactome**
748 **Genes in the Epidermal Epithelium**
749

750 **Table S2. *Drosophila* Genotypes**
751

752 **Table S3. Statistical Comparisons of Lrrk Inhibition and ATP7 Down-regulation Viability**
753
754 **Table S4. Statistical Comparisons of Glucose Treated Lrrk and ATP7 Down-regulation or**
755 **Over-expression Survival**
756
757 **Table S5. Statistical Comparisons of Copper Treated Lrrk and ATP7 Down-regulation**
758 **Survival**
759
760 **Table S6. Statistical Comparisons of Lrrk Inhibition and ATP7 Over-expression Viability**
761
762 **Table S7. Statistical Comparisons of Copper Treated Lrrk and ATP7 Over-expression**
763 **Survival**
764
765
766
767
768
769

Females

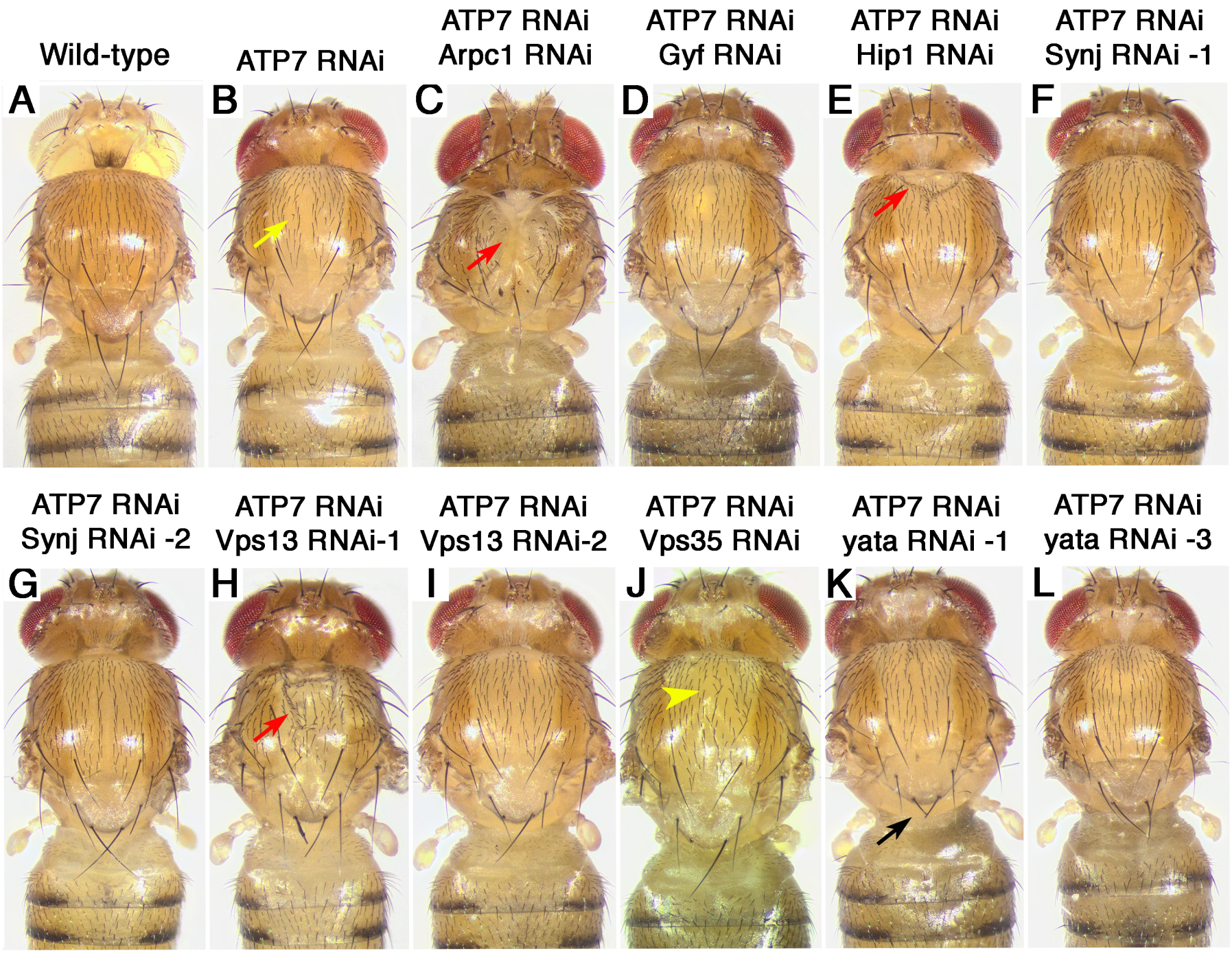

Figure 1

Males

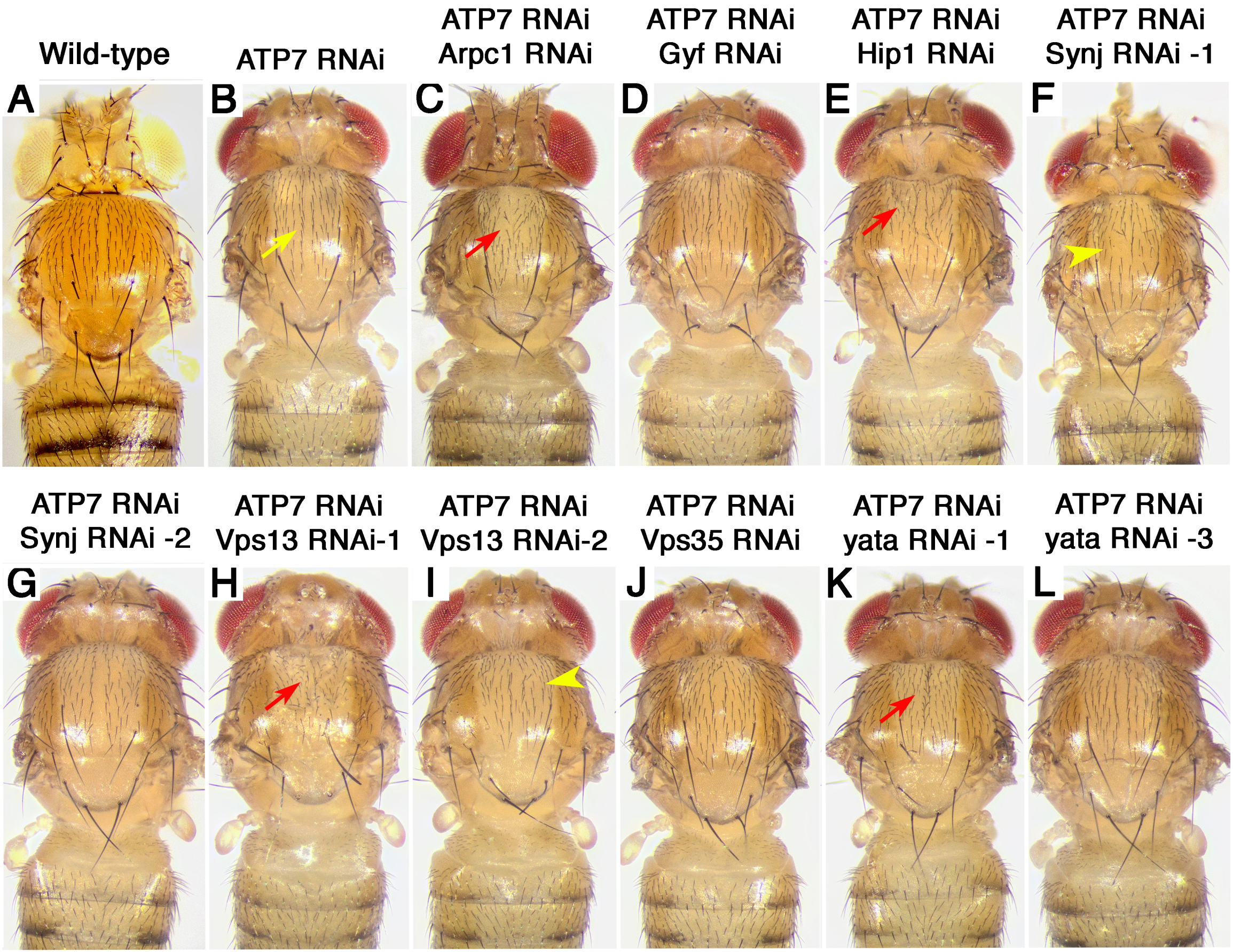

Figure 2

Females

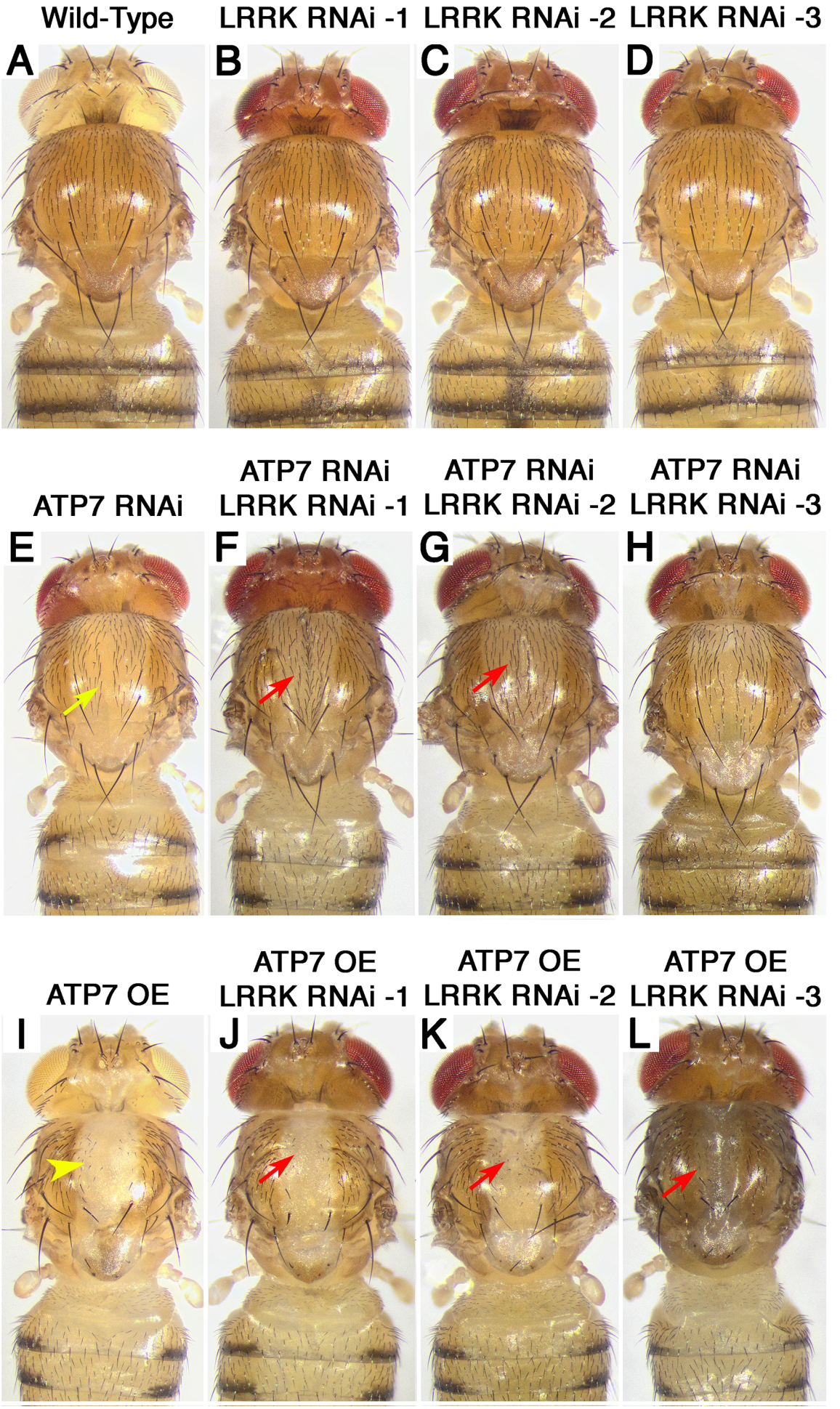

Figure 3

Males

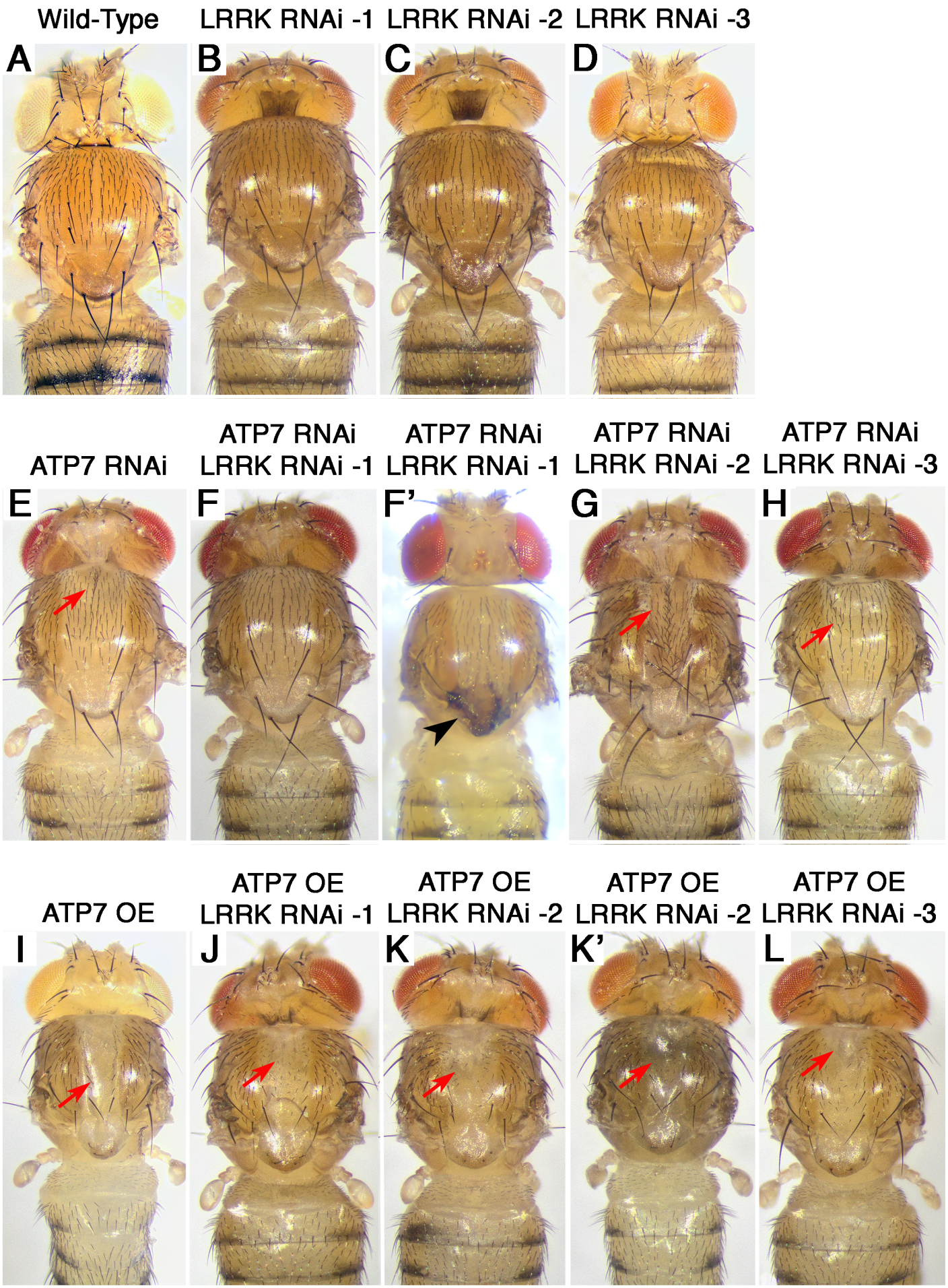

Figure 4

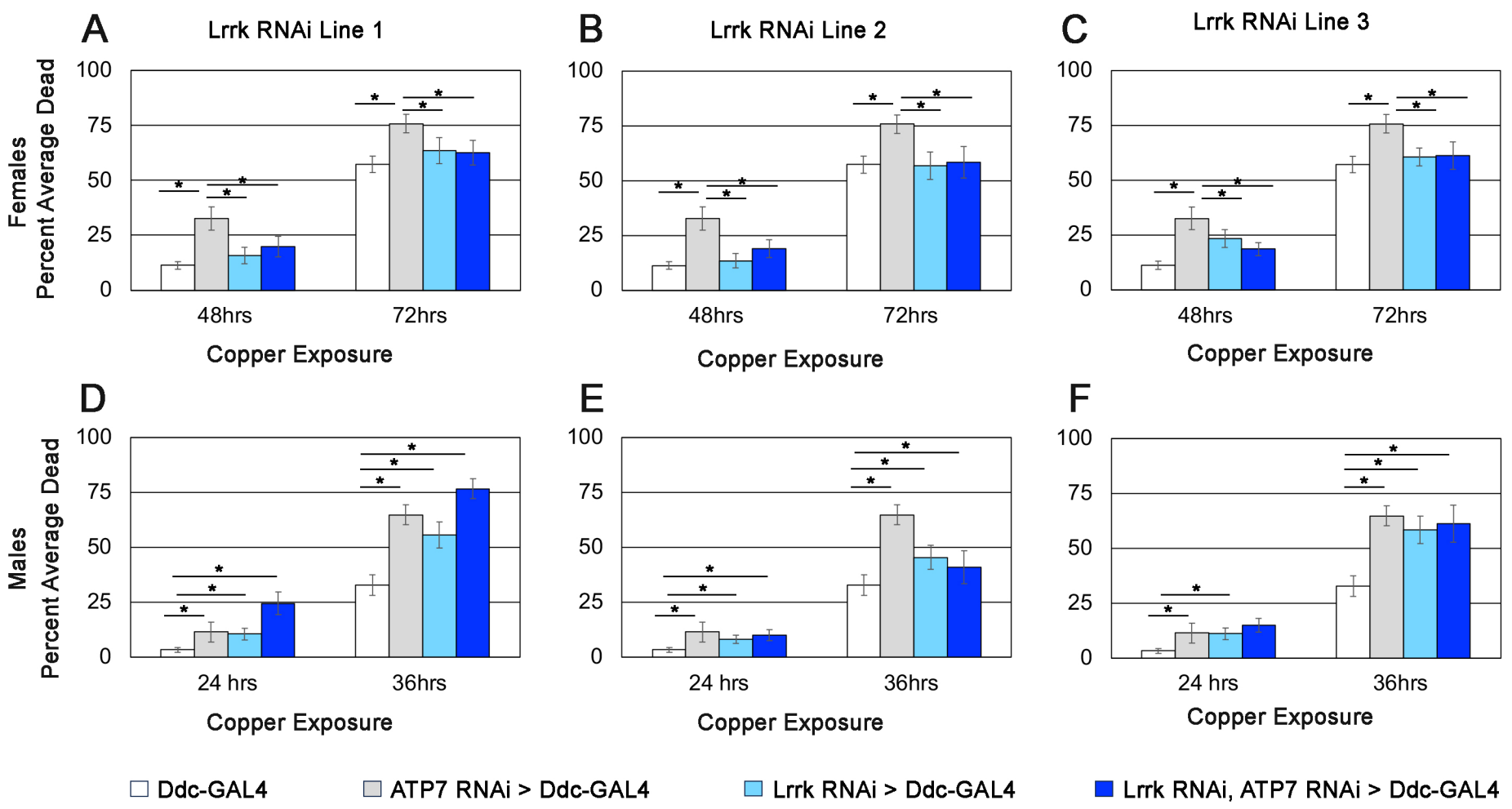
A
Lrrk RNAi Line 1
B
Lrrk RNAi Line 2
C
Lrrk RNAi Line 3
Females
Percent Average Dead
100
75
50
25
0
48hrs
72hrs
Copper Exposure
D
E
F
Males
Percent Average Dead
24 hrs
36hrs
Copper Exposure
Ddc-GAL4
ATP7 RNAi > Ddc-GAL4
Lrrk RNAi > Ddc-GAL4
Lrrk RNAi, ATP7 RNAi > Ddc-GAL4

Figure 5

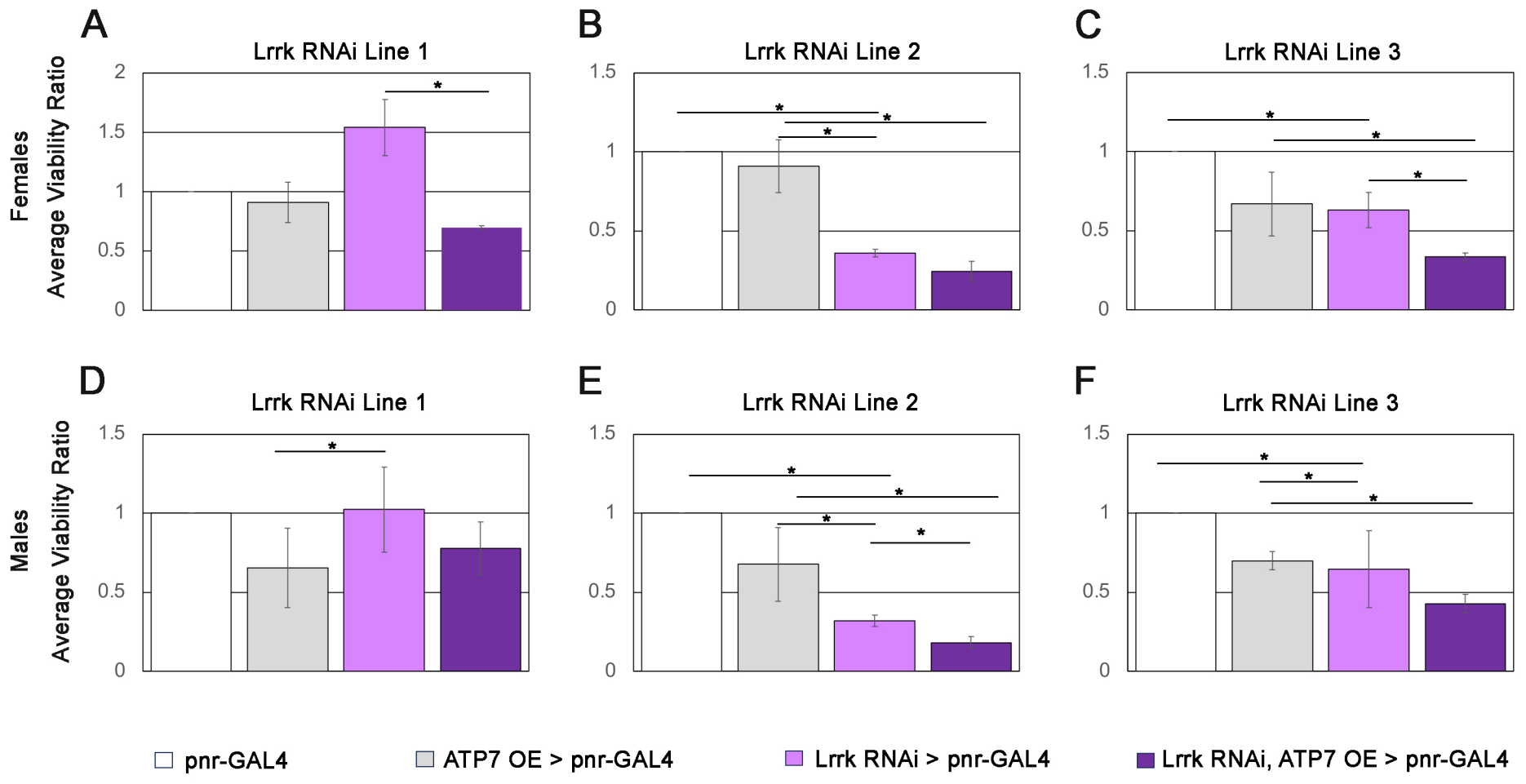
A
Lrrk RNAi Line 1
B
Lrrk RNAi Line 2
C
Lrrk RNAi Line 3
D
Lrrk RNAi Line 1
E
Lrrk RNAi Line 2
F
Lrrk RNAi Line 3
Females
Males
Average Viability Ratio
0
0.5
1
1.5
2
*
pnr-GAL4
ATP7 OE > pnr-GAL4
Lrrk RNAi > pnr-GAL4
Lrrk RNAi, ATP7 OE > pnr-GAL4

Figure 6

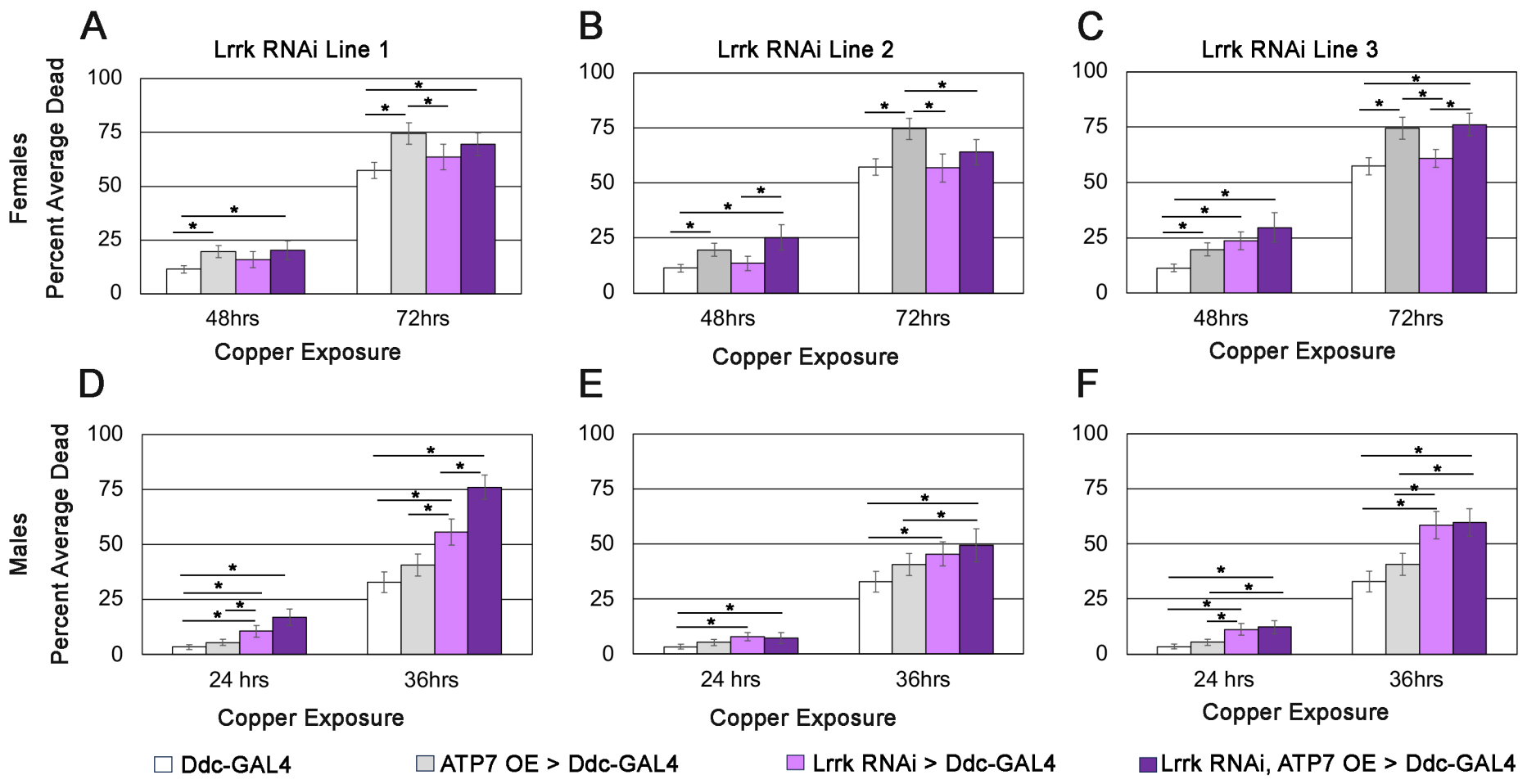
A
Lrrk RNAi Line 1
B
Lrrk RNAi Line 2
C
Lrrk RNAi Line 3
Females
Percent Average Dead
100
75
50
25
0
48hrs
72hrs
Copper Exposure
D
E
F
Males
24 hrs
36hrs
Ddc-GAL4
ATP7 OE > Ddc-GAL4
Lrrk RNAi > Ddc-GAL4
Lrrk RNAi, ATP7 OE > Ddc-GAL4

Figure 7

Drosophila Candidate Gene	Drosophila Gene Abbreviation	Human Homolog Gene Name	Human Homolog Abbreviation	OMIM Number	PARK Number
Actin-related protein 2/3 complex, subunit 1	Arpc1	Actin-Related Protein 2/3 Complex	ARPC1	604223	N/A
Gigyf	Gyf	GRB10 interaction GYF protein 2	GIGYF2	607688	N/A
Huntingtin interacting protein 1	Hip1	Huntingtin interacting protein 1	HIP1	601767	PARK11
Leucine-rich repeat kinase	Lrrk	Leucine rich repeat kinase 2	Lrrk2	607060	PARK8
Synaptojanin	Synj	Synaptojanin 1	Synj1	615530	PARK20
Vacuolar protein sorting 13	Vps13	Vacuolar protein sorting 13C	VPS13C	616840	PARK23
Vacuolar protein sorting 35	Vps35	VPS35 retromer complex component	VPS35	601501	PARK17
yata	yata	SCYL like pseudokinase 1	SCYL1	616719	N/A

Table 1. *Drosophila* Homologues of ATP7A Interactome Genes